ENHANCING ROBUSTNESS OF VISION-LANGUAGE MODELS THROUGH ORTHOGONALITY LEARNING AND SELF-REGULARIZATION

Anonymous authors
Paper under double-blind review

ABSTRACT

Efficient fine-tuning of vision-language models (VLMs) like CLIP for specific downstream tasks is gaining significant attention. Previous works primarily focus on prompt learning to adapt the CLIP into a variety of downstream tasks, however, suffering from task overfitting when fine-tuned on a small data set. In this paper, we introduce an orthogonal fine-tuning method for efficiently fine-tuning pretrained weights and enabling enhanced robustness and generalization, while a self-regularization strategy is further exploited to maintain the stability in terms of zero-shot generalization of VLMs, dubbed ***OrthSR***. Specifically, trainable orthogonal matrices are injected seamlessly into the transformer architecture and enforced with orthogonality constraint during the training, benefiting from the norm-preserving property and thus leading to stable and faster convergence, while keeping the pre-trained weights frozen. To alleviate deviation from fine-tuning, a self-regularization strategy is further employed to retain the generalization of the model during the training within a bypass manner. In addition, to enrich the sample diversity for downstream tasks under the small dataset scenario, we first explore attentive CutOut data augmentation to boost the efficient fine-tuning, leading to better model fitting capacity for specific downstream task. Then we support the theoretical analysis on how our approach improves the specific downstream performance and maintains the generalizability. For the first time, we revisit the CLIP and CoOp with our method to effectively improve the model on few-shot image classficiation scenario on par with the elaborated prompt learning methods. We conduct extensive experiments to demonstrate that our method explicitly steers pretrained weight space to represent the task-specific knowledge and presents competitive generalizability under *base-to-base/base-to-new*, *cross-dataset transfer* and *domain generalization* evaluations.

1 INTRODUCTION

Large-scale pre-trained vision-language models (VLMs) have been emerging as prevalent cornerstones in a wide spectrum of downstream vision and vision-language tasks, including few-shot image recognition [90; 91; 88; 22; 38; 92; 70; 57; 12; 77], object-detection [21; 25; 3; 85] and segmentation [18; 6; 67; 79]. Leading models like CLIP [66] and ALIGN [36] demonstrate remarkable generalizability by training with aligning image-text pairs from large web corpora using contrastive loss, thereby encoding open-vocabulary concepts within a joint vision-language embedding space. Despite the effectiveness of these VLMs in zero-shot recognition, fine-tuning them for specific downstream tasks while preserving their strong zero-shot capabilities remains a significant challenge. Designing manual text prompts for different tasks requires substantial human effort and expert knowledge, which is often infeasible for achieving optimal performance in data-efficient settings [8].

Recently, prompt learning [91; 90] serves as an exceptional paradigm to achieve this objective, however, tending to prioritize task-specific knowledge and resulting in task overfitting issues [61; 39], where the fine-tuned model struggles to generalize well to *new/unseen* tasks under data-efficient settings. To address this dilemma, alternative approaches must be explored. Drawing inspiration from empirical observations that hyperspherical similarity effectively encodes semantic information [9; 53; 51] and that hyperspherical energy [52] can characterize the pairwise relational structure among

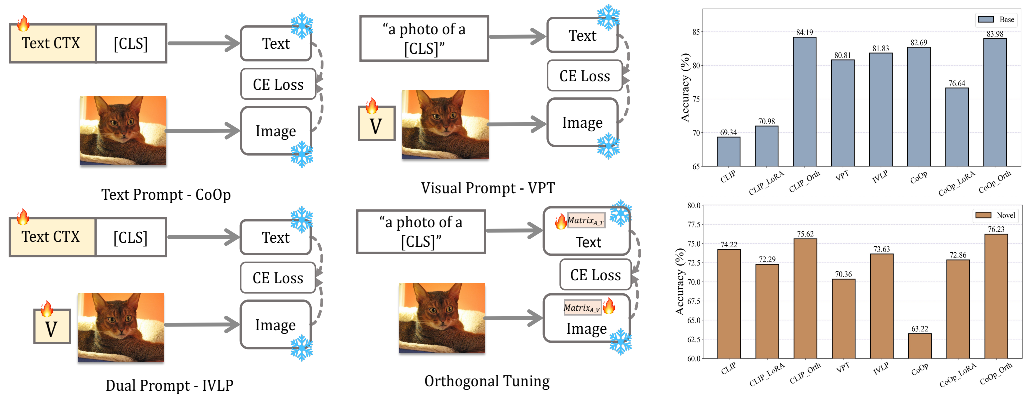

(a) Tuning paradigm comparison (b) Base and novel evaluation

Figure 1: The pipeline comparison for tuning or adapting VLMs into downstream tasks. Our contribution is to introduce a new fine-tuning pipeline by orthogonal tuning, that boost the CLIP and CoOp with competitive base/novel accuracy performances when compared with existing methods (results are computed by average 11 datasets).

neurons, we hypothesize that well-pretrained models like CLIP should maintain consistent levels of hyperspherical energy even after fine-tuning. An intuitive approach is to use a suitable regularizer to preserve hyperspherical energy levels during the fine-tuning phase. However, ensuring that the difference in hyperspherical energy is minimized remains a challenge. Inspired by recent orthogonal transformation methods [65; 54], we propose that the pretrained pairwise hyperspherical energy can be preserved by leveraging orthogonal transformation for all neurons with the same operation. This approach utilizes the invariance property of orthogonal transformation, meaning norm-preserving during fine-tuning, to maintain consistent hyperspherical energy levels.

Motivated by the preservation of hyperspherical energy through orthogonal transformation, we introduce Orthogonality Learning to adapt pretrained VLMs (*e.g.,* CLIP) to specific downstream tasks (*e.g.,* few-shot image recognition) without altering their hyperspherical energy, thanks to the norm-preserving property during fine-tuning. This approach differs from common methods that heavily rely on prompt learning. Furthermore, previous works [48; 52; 54] have shown that small hyperspherical energy leads to better generalization, and orthogonal transformation is a suitable and flexible solution for achieving this, especially in classification task. Our main idea is to apply the same orthogonal transformation to neurons so that pairwise angles are maintained within the hypersphere of CLIP. Although prevalent adaptation methods for pretrained weights, such as LoRA [33], achieve fine-tuning by adding small component matrices, they still suffer from low training convergence and generalizability degradation.

In this paper, we propose a novel and efficient fine-tuning method using **Orth**ogonality Learning, motivated by the preservation of hyperspherical energy through orthogonal transformation, shown different paradigm with exisitng works in Fig. 1 (a). To mitigate deviation from orthogonal constraint during training, we introduce a **S**elf-**R**egularization strategy using the initial pretrained weights as an *anchor* point, thus dubbed ***OrthSR***. Our method keeps the pretrained weights frozen while applying orthogonal fine-tuning and regularization simultaneously. In the dual-branch transformer architecture of the CLIP model, we inject trainable orthogonal matrices and enforce orthogonal constraints (such as using Cayley parameterization [29; 43]). This ensures each injected layer matrix is orthogonal with a determinant of 1. We investigate orthogonal fine-tuning in both image and text encoder of CLIP to demonstrate training efficiency and generalizability preservation of our method, distinguishing it from prompt tuning and low-rank matrix decomposition methods. The norm-preserving property of orthogonal transformations helps maintain hyperspherical energy levels, benefiting of stable convergence, robustness, and generalization. This enables seamless integration of task-specific knowledge into pretrained VLMs, allowing the trainable matrices to be merged with frozen weights during deployment without adding inference latency, while we shows evaluation superiority over previous methods in Fig. 1 (b). To prevent significant deviations from the pretrained model, we employ a Self-Regularization strategy that guides the model to stay close to the *anchor* point, supported by the pretrained model within a bypass manner. This simple yet effective approach sustains orthogonal fine-tuning with initial *anchor* regularization, avoiding deviations from the zero-shot generalizability manifold severely. Besides, we utilize attentive CutOut data augmentation to enrich the data diversity, enhancing the task-specific knowledge of fine-tuned model (*e.g.,* few-shot image recognition) under data-efficient setting. This leads to better model fitting capacity for specific downstream task, serving as implicitly increasing the sample diversity. Unlike previous works [65; 54], we focus on adapting VLMs to high-level task-specific scenarios (*e.g.,* recognition) rather than fine-tuning generative models. Additionally, we devise a suitable regularization strategy to retain the strong generalizability that elucidates the training efficiency and generalizability preservation of our method.

Extensive experiments demonstrate the effectiveness of our ***OrthSR*** by evaluating on representative benchmarks: *base-to-base/base-to-new, cross-dataset transfer and domain generalization*. In the *base-to-base/base-to-new* setting, our method improves the new class of baseline model by 13.3% on average across 11 datasets, by 0.95% for *cross-dataset* setting and 1.80% on average across the four datasets for *domain generalization* setting, all of which presents competitive performance over the existing SoTAs. In summary, our contributions can be summarized as follows:

- We introduce a novel and efficient orthogonal fine-tuning method to adapt the VLMs into task-specific knowledge while maintaining strong generalizability. Due to the norm-preserving property, this fine-tuning leads to stable and faster convergence and exhibits superiority over the prompt tuning methods.
- To further mitigate the deviation from the pretrained model, we design a Self-Regularization strategy to enforce the fine-tuned model distilling informative zero-shot generalization information of the pretrained logits.
- Attentive CutOut data augmentation is employed to enhance the task-specific knowledge when fine-tuning the VLM under data-efficient setting.
- Extensive experiments are conducted to validate the effectiveness and effciency of our method, for the first time, we boost the CLIP and CoOp with weight decomposition tuning to obtain on par or even superior performances over existing methods.

2 Related works

Vision language models. Recently, with a significant upsurge of large-scale pretrained vision-language models (VLMs) [84; 89; 36; 13; 66; 74], text and image embeddings have been trained jointly to be aligned with the large-scale image-text pairs corpora. Driven by contrastive loss in a self-supervised manner, VLMs like CLIP [66], ALIGN [36], LiT [87], FLIP [47] and Florence [84] have elucidated remarkable performance. For instance, CLIP [66] and ALIGN [36] utilize approximately 400 million and 1 billion image-text pairs, respectively, to accomplish their multi-modal alignment training, benefiting a wide spectrum of downstream vision and vision-language tasks, including few-shot image-level recognition [90; 91; 88; 22; 38; 92; 70; 57; 12; 77], object detection [21; 25; 3; 85] and segmentation [18; 6; 67; 79]. Despite strong generalizability towards zero-shot recognition tasks of these VLMs, effectively transferring them to downstream tasks without degrading their inherent generalization ability remains a challenging problem.

Efficient tuning for vision language models. With the emergence of VLMs, efficiently adapting these models to specific downstream tasks with limited data samples has garnered significant interest. Prompt Tuning is firstly proposed in the NLP field [49; 23; 46; 42], which attempts to learn task-specific prompt templates. Recently, in the computer vision community, CoOp [91] pioneers the study by tuning the contextual tokens in text branch of CLIP into a set of learnable tokens to few-shot image recognition, which is further improved by CoCoOp [90] through a Meta-Network [58] paradigm to address the overfitting issue on base classes while generalizing better on unseen classes. To efficiently adapt large pretrained Vision Transformers, VPT [37] and Visual Prompting [2] both insert trainable tokens into the input space of transformer model. To leverage additional prompt learning for dual-branch models like CLIP, a plethora of works [38; 39; 14; 86; 61; 92; 55; 77] have been proposed to learn these prompts towards a way that treats them as *continuous* learnable vectors while keeping the original model parameters frozen to retain the strong generalizability. Very recently, Test-Time Prompting [71; 70] emerges with the objective of enforcing consistency regularization between multiply views of a test sample by minimizing their averaged entropy. Another line of work [8; 17; 27] focuses on tuning VLMs over the pretrained weights. Adaptation methods [32; 33; 63] have become increasingly ubiquitous. The LoRA series [33; 50; 16] is widely used to finetune pretrained model weights using low-rank matrix optimization. Our method shares a similar principle with LoRA for adapting pretrained model weights, but introduces a novel Orthogonality Learning approach. This not only enhances performance for specific downstream tasks (*e.g.,* few-shot recognition) but also improves robustness and generalization with more efficient convergence.

Orthogonality regularization. Orthogonality has been commonly adopted to introduce orthogonal regularization to improve the robustness of Deep Neural Networks [51; 7; 35; 83; 34; 43; 1; 80; 64; 45], that norm-preserving property can avoid exploding or vanishing gradients during training [4; 24], leading to faster convergence and encouraging robustness and generalization. This objective can be reached by a simple Cayley parameterization [29; 43]. Recently,OPT [54] introduces an orthogonal transformation applied to the neural weights to maintain the minimum hyperspherical energy. Furthermore, OFT [65] extend this orthogonal paradigm to finetune the text-to-image diffusion models by employing Cayley parameterization constraint during the finetuning. In this paper, we further explore the utilization of orthogonal finetuning on CLIP for specific downstream tasks while proposing different regularization strategies to enhance generalizability on *novel/uneen* classes.

3 METHODOLOGY

3.1 PRELIMINARIES

Contrastive Language-Image Pre-training (CLIP). CLIP consists of two parallel encoders, image and text encoders, represented by $\theta_{CLIP} = \{\theta_v, \theta_t\}$. The image encoder $\mathcal{F}_v$ can be either a CNN [26] or a ViT [75; 19] for mapping input image into a image embedding, and the text encoder $\mathcal{F}_t$ is a Transformer [17] for mapping input text into a text embedding, respectively. During pre-training, CLIP utilizes two parallel encoders to separately encode image and text into corresponding vectors in jointly aligned embedding space, and then adopts contrastive loss to pull together the cosine similarities of the correct image-text vector pairs while pushing away the cosine similarities of incorrect pairs. After pretrained on large-scale image-text pairs corpora, CLIP is capable of computing the text-image similarity and can be generalized to downstream tasks, like zero-shot image recognition, without fine-tuning. Specifically, the input image X is first divided into M patches and then projected into patch tokens, and a global class token $[CLS]$ is prepended to the patch token sequence, obtaining $X_0 = \{CLS, e_1, e_2, ..., e_M\}$ where e_i standds for the i^{th} patch. Those patch tokens will be encoded by transformer blocks inside the image encoder $\mathcal{F}_v$ by $f_v = \mathcal{F}_v(X_0 : \theta_v)$. Given the labels $\{[class]_c\}_{c=1}^{C}$ for the C categories for classification where $[class]_c$ represents the class name of the c^{th} class, a hand-crafted text prompt like 'a photo of a $[CLS]$' will be embedded within the class label $[class]_c$ This results in $\mathcal{Y}_0 = \{SOS, t_1, t_2, ..., t_L, c_k, EOS\}$ where SOS and EOS denote the start and end token embeddings while t_i and c_k are specific word embedding corresponding to the text prompt and the class label, respectively. The text encoder $\mathcal{F}_t$ will encode $\mathcal{Y}_0$ via transformer blocks to produce text feature embeddings as $f_t = \mathcal{F}_t(\mathcal{Y}_0 : \theta_t)$. During zero-shot inference, the prediction probability on image X will be computed as $p(y_i|X) = \frac{exp(sim(f_t \cdot f_v)/\tau)}{\sum_{i=1}^{C} exp(sim(f_t \cdot f_v)/\tau)}$, where τ is a learned temperature coefficient and sim denotes the cosine similarity computation, respectively.

Context Optimization (CoOp) [91] proposes to leverage tunable text prompt by replacing the cumbersome and fixed hand-crafted prompt, that can be learnt from data. Now, the tunable prompt is constructed with M learnable *continues* context vectors as $w = \{w_1, w_2, ..., w_M, c_k\}$, where w_i represents the i^{th} tunable vector and c_k denotes the c^{th} class name $[class]_c$. The finally fine-tuned training objective of CoOp is to optimize the contextual vectors w_i only by minimize the cross-entropy loss between the ground-truth $\hat{y}$ and the model prediction y as:

$$p(y_i|X) = \frac{exp(sim(f_t(:w) \cdot f_v)/\tau)}{\sum_{i=1}^{C} exp(sim(f_t(:w) \cdot f_v)/\tau)}, \quad \mathcal{L}_{\text{ce}} = -\log p(\hat{y} = y|X) \tag{1}$$

3.2 ORTHOGONAL FINE-TUNING

Traditionally, fine-tuning VLMs into specific downstream scenarios typically embraces small learning rate with gradient descent optimizer to update the model, This scheme implicitly constrains risky deviation from pretrained model, aiming to finetune the model via implicitly minimizing $\|\boldsymbol{M} - \boldsymbol{M}_0\|$ where $\boldsymbol{M}$ is the fine-tuned model weights and $\boldsymbol{M}_0$ is the pretrained model weights. Towards this strategy, there are still various ways to finetune a pretrained VLM. For example, LoRA [33] employs

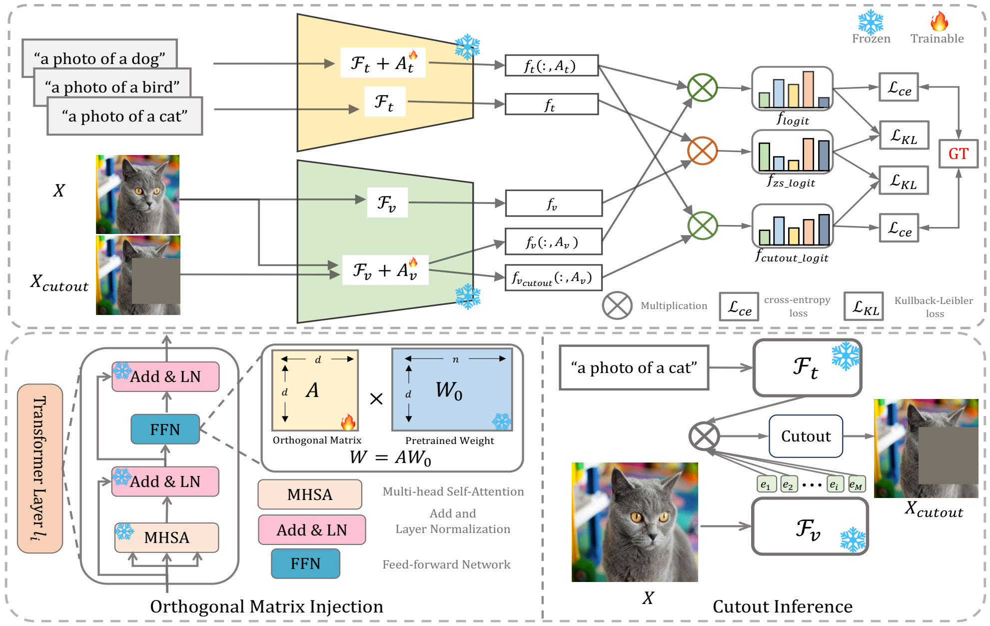

Figure 2: Overview of our proposed pipeline, ***OrthSR***. The top shows our fine-tuning pipeline by applying orthogonal tuning into the Feed-Forward-Network of both image and text encoder ($\mathcal{F}_v$ and $\mathcal{F}_t$) of CLIP model which is trained with Self-Regularization strategy. On the left of bottom, orthogonal matrix injection is explained by injecting orthogonal matrix into the pretrained weights with orthogonalization constraint (such as Cayley parameterization). On the right of bottom, pretrained CLIP is utilized to highlight the most-discriminative image regions and then apply cutout operation to obtain cutout image X_{cutout} which will be input to the fine-tuned model together with original X.

an additive low-rank matrix with constraint for model weights update, *i.e.,* $\text{rank}(\boldsymbol{M}-\boldsymbol{M}_0)=r'$ where r' is set to be relatively smaller number than the pretrained ones. Differently, Orthogonal transformation targets at inducing a constraint for the pairwise similarity between neurons [54; 65]: $\|\text{HE}(\boldsymbol{M})-\text{HE}(\boldsymbol{M}_0)\|=0$,where $\text{HE}(\cdot)$ denotes hyperspherical energy of a weight matrix. In this paper, we draw attention to the Feed-Forward-Networks (FFN) within the transformer architecture of CLIP, shown in Fig 2. Suppose a fully-connected layer with $\boldsymbol{W}=\{\boldsymbol{w}_1,\cdots,\boldsymbol{w}_n\}\in\mathbb{R}^{d\times n}$ where $\boldsymbol{w}_i\in\mathbb{R}^d$ is the i^{th} neuron ($\boldsymbol{W}_0$ is the pretrained weights). We expect to acquire the output vector $\boldsymbol{z}\in\mathbb{R}^n$ by $\boldsymbol{z}=\boldsymbol{W}^\top\boldsymbol{x}$ where $\boldsymbol{x}\in\mathbb{R}^d$ is the input vector. When introducing the orthogonal fine-tuning as minimizing the hysperical energy difference between the fine-tuned and pretrained model:

$$\min_{\boldsymbol{W}}\|\text{HE}(\boldsymbol{W})-\text{HE}(\boldsymbol{W}_0)\| \;\Leftrightarrow\; \min_{\boldsymbol{W}}\left\|\sum_{i\neq j}\|\hat{\boldsymbol{w}}_i-\hat{\boldsymbol{w}}_j\|^{-1}-\sum_{i\neq j}\|\hat{\boldsymbol{w}}_i^0-\hat{\boldsymbol{w}}_j^0\|^{-1}\right\| \tag{2}$$

where $\hat{\boldsymbol{w}}_i=\frac{\boldsymbol{w}_i}{\|\boldsymbol{w}_i\|}$ is the i^{th} normalized weight, and the hyperspherical energy of a fully-connected layer $\boldsymbol{W}$ is defined as $\text{HE}(\boldsymbol{W}):=\sum_{i\neq j}\|\hat{\boldsymbol{w}}_i-\hat{\boldsymbol{w}}_j\|^{-1}$. This objective can be optimally minimized to be zero. To achieve this target, we introduce the orthogonal transformation into the pretrained weights, $\boldsymbol{W}=\boldsymbol{A}\boldsymbol{W}_0$ in which $\boldsymbol{A}\in\mathbb{A}^{d\times d}$ is an orthogonal matrix, meaning that the determinant is 1 or -1 of the initial matrix by imposing rotation or reflection, respectively. Now we can formulate the forward pass of FFN from $\boldsymbol{z}=(\boldsymbol{W}_0)^\top\boldsymbol{x}$ to:

$$\boldsymbol{z}=\boldsymbol{W}^\top\boldsymbol{x}=(\boldsymbol{A}\cdot\boldsymbol{W}_0)^\top\boldsymbol{x},\quad \text{s.t. } \boldsymbol{A}^\top\boldsymbol{A}=\boldsymbol{A}\boldsymbol{A}^\top=\boldsymbol{I} \tag{3}$$

where $\boldsymbol{W}$ denotes the fine-tuned weight matrix and $\boldsymbol{I}$ is an identity matrix. During the fine-tuning, we optimize the added $\boldsymbol{A}$ while keeping the pretrained weights $\boldsymbol{W}_0$ frozen. To finetune the model from $\boldsymbol{W}_0$, we initialize the orthogonal matrix $\boldsymbol{A}$ to be identity matrix $\boldsymbol{I}$, sharing similar principle with LoRA to set zero initialization of the additive matrices. Moreover, this allows us to gradually inject task-specific knowledge into the fine-tuned model driven by cross-entropy loss.

Motivated by previous works [54; 43; 29] discussing about differential orthogonalization methods, we focus on taking utilization of Cayley parameterization. The Cayley transform produces a representation of orthogonal matrices without -1 eigenvalues using skew-symmetric matrices (*i.e.,* $\boldsymbol{C}^\top = -\boldsymbol{C}$) as follows:

$$\boldsymbol{A} = (\boldsymbol{I}+\boldsymbol{C})^{-1}(\boldsymbol{I}-\boldsymbol{C}), \boldsymbol{C} = (\boldsymbol{I}+\boldsymbol{A})^{-1}(\boldsymbol{I}-\boldsymbol{A}) \tag{4}$$

wherein we find this special orthogonal group is able to obtain competitive performances when adapting CLIP for downstream tasks (*e.g.,* few-shot image recognition). Based on the orthogonal fine-tuning above to adapt the VLM into downsream scenario, we find there exists a potential risky error bounding such that the fine-tuned model presents inferior generalizability on *new/unseen* classes, shown in our experimental part. After applying the Neumann series to analyze: $\boldsymbol{A} = (\boldsymbol{I}+\boldsymbol{C})^{-1}(\boldsymbol{I}-\boldsymbol{C})$ can be written as: $\boldsymbol{A} \approx \boldsymbol{I} + 2\boldsymbol{C} + \mathcal{O}(\boldsymbol{C}^2)$, We empirically observe that this approximation results in instability of the fine-tuning [72], which degrades the zero-shot generalization of the pretrained model, showing different phenomena with previous work [65] on fine-tuning generative models.

3.3 SELF-REGULARIZATION

This inspires us to investigate the regularization strategy to carefully constrain the fine-tuned model not deviating far away from the pretrained one. Therefore, we further design a Self-Regularization strategy to regularize the fine-tuned model through pretrained model with a bypass manner since the pretrained weights are frozen. As shown in Fig 2, the text prompts are processed by frozen text encoder $\mathcal{F}_t$ to obtain text embedding f_t, while we can also compute new text embedding $f_t(:, A_t)$ which is encoded by orthogonal tuning text encoder after injecting orthogonal matrix to each FFN layer, $\mathcal{F}_t + A_t$. Here, we want to optimize the additive A_t for the text encoder. At the same time, we input original image to the image encoder, and obtain f_v encoded by frozen $\mathcal{F}_v$ and $f_v(:, A_v)$ from $\mathcal{F}_v + A_v$, enabling A_v tunable only. Further, the pretrained and fine-tuned logit are computed as follows:

$$f_{zs\_logit} = sim(f_t \cdot f_v), \quad f_{logit} = sim(f_t(:, A_t) \cdot f_v(:, A_v)) \tag{5}$$

Then, we adopts the cross-entropy loss to train the model given the class label $\hat{y}$ as:

$$p(y_i|X) = \frac{exp(sim(f_t(:, A_t) \cdot f_v(: A_v))/\tau)}{\sum_{i=1}^{C} exp(sim(f_t(:, A_t) \cdot f_v(:, A_v))/\tau)}, \quad \mathcal{L}_{\text{ce}} = -\log p(\hat{y} = y|X) \tag{6}$$

To further impose regularization from the pretrained *anchor* point,Then *Kullback-Leibler* loss $\mathcal{L}_{kl}$ is used to distill informative zero-shot knowledge from the *anchor* point so as to alleviate deviation far away from the pretrained mainfold wthin a bypass manner, as follows:

$$\mathcal{L}_{kd} = \mathcal{D}_{kd}(f_{logit}, f_{zs\_logit}) \tag{7}$$

where $\mathcal{D}_{kd}(f_{logit}||f_{zs\_logit}) = \sum\limits_{x \in X}(g(f_{logit})log\frac{g(f_{logit})}{g(f_{zs\_logit})}))$, $g(\cdot)$ denotes softmax function.

3.4 CUTOUT AUGMENTATION

As shown in Fig 2, we utilize the pretrained model to infer the similarity map by computing the cosine similarity between image patch tokens and $[CLS]$ text token, named as attentive CutOut. Then it produces a map that each patch responses to $[CLS]$ text token and then reshape them into the same shape of the input image. During the training, we randomly select a cutout region size to zero the top-K image patches, where K ranges from $[l, L]$. To enforce randomness to image encoder so that the model can pay more attention to other less-discriminative image regions, we generate random and different erasing size for each training iteration. Specifically, let X_{cutout} be the cutout image. We input it into the image encoder with $\mathcal{F}_v + A_v$ and obtain $f_{v\_cutout}(:, A_v)$. After that, following the aforementioned way, we then calculate the cutout logit f_{cutout_logit} as:

$$f_{cutout\_logit} = sim(f_t(:, A_t) \cdot f_{v\_cutout}(:, A_v)) \tag{8}$$

Similarly, we acquire the cutout classification and Kullback-Leibler loss in terms of the cutout image X_cutout as:

$$\mathcal{L}_{\text{cutout\_ce}} = -\log p(\hat{y} = y|X_{cutout}), \quad \mathcal{L}_{cutout\_kd} = \mathcal{D}_{kd}(f_{cutout\_logit}, f_{zs\_logit}) \tag{9}$$

In this way, we enforce the fine-tuned model pay more attention to other less-discriminative image regions that response weak to the text embedding but still contains informative cues to help model learn task-specific knowledge under the data-efficient setting, which serves as diversifying samples.

3.5 Training objective

Overall, the training losses of our method consist of two parts, one for the image classification loss including global image classification loss and cutout image classification loss, while the other one includes two corresponding distillation loss. We expect that introducing orthogonal tranformation into CLIP model fine-tuned for specific downstream tasks is able to retain strong generalizability preservation. Hence, the overall loss $\mathcal{L}_{final}$ can be written as:

$$\mathcal{L}_{\text{final}} = \lambda_1(\mathcal{L}_{ce} + \mathcal{L}_{cutout\_ce}) + \lambda_2(\mathcal{L}_{kd} + \mathcal{L}_{cutout\_kd}) \tag{10}$$

where λ_1 and λ_2 are loss balancing hyper-parameters, weighting the task-agnostic and task-specific knowledge learning.

3.6 Theoretical Analysis

In this section, we provide theoretical analysis for the generalization error bound of *OrthSR*.

We define the following optimization objectives according to Eq. 10:

$$\min_{\Theta\in\mathbb{R}} \underbrace{\frac{1}{N}\sum_{i=1}^{N}\mathcal{L}\left(\hat{s}_i^S\left(\Theta\right), y_i^{gt}\right)}_{\mathcal{L}_{CE}} + \lambda\underbrace{\mathcal{L}\left(\hat{s}^S\left(\Theta\right), \hat{s}^T\right)}_{\mathcal{L}_{KD}}, \tag{11}$$

where Θ represents learnable orthogonal matrices $\{A_v, A_t\}$ of the proposed method, and we use S and T here to denote the fine-tuned model and pre-trained *anchor* model. Now we further analyze the effectiveness of *OrthSR* by computing the generalization error bound. This bound computes the bias between the generalization error $\varepsilon\left(\Theta\right) := \mathbb{E}_{(\hat{s}^S, y^{gt})\sim\mathcal{D}}\mathcal{L}\left(\hat{s}^S\left(\Theta\right), y^{gt}\right)$ and empirical error $\bar{\varepsilon}_{\chi}\left(\Theta\right) := \frac{1}{N}\sum_{i=1}^{N}\mathcal{L}\left(\hat{s}_i^S\left(\Theta\right), y_i^{gt}\right)$, where D is the real data distribution and $\mathbb{E}\left(\cdot\right)$ denotes the expectation function.

Theorem 1. *Assume that Θ^* is the solution to Eq. equation 11. Then we have that for any $0 < \epsilon < 1$ with probability $1 - \epsilon$,*

$$\epsilon(\Theta^*) - \bar{\epsilon}_{\chi}(\Theta^*) \leq X^*\sqrt{\frac{2\ln(1/\delta)}{N}} + \frac{C''}{\lambda^{2\alpha}\sqrt{N}}.$$

where $X^* = \max_{r\in\mathbb{N}_N}\left|\mathcal{L}\left(\hat{s}_r^S\left(\Theta\right), y_r^{gt}\right)\right|$ and $\alpha > 0$.

The first term of the upper bound converges with the increasing of the number of training data N, that can be achieved by our proposed attentive CutOut data augmentation instead of using extra data. We can also find that the second term converges to 0 with the increasing of λ, which means the our self-regularization $\mathcal{L}_{KD}$ within a bypass manner effectively improves the generalization ability of our method.

4 Experiments

4.1 Experimental settings

Datasets: For evaluation in terms of both *base-to-base* and *base-to-new* class generalization, we conduct our method on publicly available 11 image recognition datasets: ImageNet [69] and Caltech101 [20] for generic objects classification, Oxford_Pets [62], StanfordCars [40], Flowers102 [60], Food101 [5] and FGVCAircraft [56] for fine-grained classification, SUN397 [82] for scene recognition, DTD [15] for texture classification, EuroSAT [28] for satellite imagery recognition and UCF101 [73] for action recognition. Following the existing methods [90; 38; 39; 14; 86; 61; 92; 55; 77], we also evaluate our method on *cross-dataset transfer* and *domain generalization*. For *cross-dataset transfer*, we adopt ImageNet as the source and the remaining 10 datasets as target

Table 1: Performance for base-to-base/base-to-new on 11 datasets. We train our model with a subset of the classes (base classes) in a 16-shot setting and evaluate on the test set including base classes and new classes, while HM denotes the harmonic mean of base and novel performance to show the generalization trade-off [81], HM=(2 $\times$ base $\times$ new)/(base + new). The highest results are highlighted in **Bold**.

Dataset		CLIP [66]	CoOp [91]	CoCoOp [90]	MaPLe [38]	RPO [41]	PLOT [10]	PromptSRC [39]	UNIGRAM [44]	VPT (Base)	IVLP (Base)	***OrthSR* (Ours)**	Gain Δ
Average on 11 datasets	Base	69.34	82.69	80.47	82.28	81.13	77.20	**84.26**	80.34	80.81	81.83	84.16	+1.47
	New	74.22	63.22	71.69	75.14	75.00	60.38	76.10	75.92	70.36	73.63	**76.55**	+13.3
	HM	71.70	71.66	75.83	78.55	77.78	67.76	79.97	78.07	74.68	77.10	**80.02**	+8.36
ImageNet	Base	72.43	76.47	75.98	76.66	76.60	75.97	77.60	76.60	70.93	76.80	**78.10**	+1.63
	New	68.14	67.88	70.43	70.54	**71.57**	69.23	70.73	70.69	65.90	70.40	70.35	+2.47
	HM	70.22	71.92	73.10	73.47	74.00	72.44	74.01	73.53	68.32	73.46	**74.02**	+2.10
Caltech 101	Base	96.84	98.00	97.96	97.74	97.97	96.53	98.10	98.07	97.86	97.53	**98.17**	+0.17
	New	94.00	89.81	93.81	94.36	94.37	82.86	94.03	**95.11**	93.76	93.57	94.03	+4.22
	HM	95.40	93.73	95.84	96.02	96.03	89.17	96.02	**96.57**	95.77	95.51	96.06	+2.33
Oxford Pets	Base	91.17	93.67	95.20	95.43	94.63	93.45	95.33	94.94	94.81	95.50	**95.60**	+1.95
	New	97.26	95.29	97.69	97.76	97.50	79.76	97.30	97.94	96.00	**97.97**	97.70	+2.41
	HM	94.12	94.47	96.43	96.58	96.05	86.06	96.30	96.42	95.40	**96.72**	96.64	+2.17
Stanford Cars	Base	63.37	78.12	70.49	72.94	73.87	61.41	78.27	73.50	72.46	73.27	**79.40**	+1.28
	New	74.89	60.40	73.59	74.00	**75.53**	42.69	74.97	75.38	73.38	74.17	73.87	+13.4
	HM	68.65	68.13	72.01	73.47	74.69	50.37	**76.58**	74.43	72.92	73.72	76.54	+8.41
Flowers 102	Base	72.08	97.60	94.87	95.92	94.13	95.62	**98.07**	95.20	95.39	96.47	97.60	+0.00
	New	**77.80**	59.67	71.75	72.46	76.67	56.03	76.50	76.21	73.87	72.90	75.53	+15.8
	HM	74.83	74.06	81.71	82.56	84.50	70.56	**85.95**	84.65	83.26	83.04	85.16	+11.1
Food101	Base	90.10	88.33	90.70	90.71	90.33	88.45	90.67	**90.84**	89.88	90.47	90.50	+0.40
	New	91.22	82.26	91.29	92.05	90.83	85.28	91.53	**92.12**	87.76	91.97	91.17	+8.91
	HM	90.66	85.19	90.99	91.38	90.58	86.84	91.10	**91.48**	88.81	91.21	90.83	+5.64
FGVC Aircraft	Base	27.19	40.44	33.41	37.44	37.33	29.63	**42.73**	32.25	33.10	34.20	41.93	+1.49
	New	36.29	22.30	23.71	35.61	34.20	16.17	**37.87**	38.00	30.49	34.00	36.87	+14.5
	HM	31.09	28.75	27.74	36.50	35.70	20.92	**40.15**	34.89	31.74	34.10	39.24	+10.4
SUN397	Base	69.36	80.60	79.74	80.82	80.60	78.56	**82.67**	80.43	79.66	81.00	82.47	+1.87
	New	75.35	65.89	76.86	78.70	77.80	72.34	78.57	77.91	72.68	78.40	**79.33**	+13.4
	HM	72.23	72.51	78.27	79.75	79.18	75.32	80.52	79.15	76.01	79.68	**80.87**	+8.36
DTD	Base	53.24	79.44	77.01	80.36	76.70	69.87	**83.37**	73.62	79.15	79.50	82.40	+2.96
	New	59.90	41.18	56.00	59.18	62.13	53.63	62.97	62.38	50.76	50.10	**65.33**	+24.1
	HM	56.37	54.24	64.85	68.16	68.61	60.68	71.75	67.56	61.85	61.47	**72.88**	+18.6
EuroSAT	Base	56.48	92.19	87.49	**94.07**	86.63	87.39	92.90	86.26	93.01	91.30	93.27	+1.08
	New	64.05	54.74	60.04	73.23	68.97	67.63	73.90	71.38	54.89	68.53	**79.00**	+24.2
	HM	60.03	68.69	71.21	82.35	76.79	74.30	82.32	78.12	69.04	78.29	**85.54**	+16.8
UCF101	Base	70.53	84.69	82.33	83.00	83.67	72.71	**87.10**	82.00	82.67	84.13	86.33	+1.64
	New	77.50	56.05	73.45	78.66	75.43	41.51	78.80	78.06	74.54	77.90	**78.87**	+22.8
	HM	73.85	67.46	77.64	80.77	79.34	52.84	**82.74**	79.98	78.39	80.90	82.43	+14.9

variants, while for *domain generalization*, we also use ImageNet as source and ImageNetV2 [68], ImageNet-Sketch [78], ImageNet-A [31] and ImageNet-R [30] as targets.

Implementation details: For all the experimental settings, we follow the common strategy of CoOp [91] and CoCoOp [90] for the fair comparison, including the dataset splits, default data augmentation, training schedule, shot of samples, backbones, length of context tokens (*i.e.,* M is 16 in this paper), *etc.* The K is set to be 3 and averaged for all the experiments, reporting base and novel class accuracy and their harmonic mean (HM), respectively. We apply CLIP-ViT-B/16 as our pretrained backbone model to train for 5 epochs with a batch size of 4, and a learning rate of 1e-5 via SGD optimizer on a single Nvidia-A100-GPU, unless other stated. The hyper-parameters λ_1 and λ_2 are set to be 1.5 and 1.2 by default, left for hyper-parameters sensitivity ablations in Appendix A.

Baseline: To validate the effectiveness of proposed ***OrthSR***, we compare our approach against the following methods, including: (1) zero-shot CLIP [66], which provides the basic baseline model for comparison without any prompt learning or adaptation finetuning; (2) commonly used single-modal prompt tuning methods to demonstrate superiority of our novel finetuning method, such as CoOp [91] which constructs another baseline model for us using tunable context vectors for the input text prompt, CoCoOp [90], PLOT [10] and UNIGRAM [44], and VPT [37]; and multi-modal prompt tuning methods: MaPLe [38] and PromptSRC [39]. Note that the original paper of PLOT [10] adopts a weaker backbone model ResNet-50 [26], here we change it to ViT-B/16 to implement for a fair comparison. Moreover, we also implement VPT which applies prompt tuning for image encoder, IVLP which applies independent prompt tuning for both image encoder and text encoder, all of which establish the basic comparisons.

Table 2: Performance comparison on the domain generalization.

	Source	Target			
	ImageNet	-V2	-S	-A	-R
CLIP	66.73	60.83	46.15	47.77	73.96
$LoRA_{CLIP}$	69.70	62.67	38.70	39.67	69.93
CoOp	71.51	64.20	47.99	49.71	75.21
CoCoOp	71.02	64.07	48.75	50.63	76.18
VPT	70.72	58.22	44.67	43.00	71.86
UPT	**72.63**	**64.35**	48.66	50.66	76.24
MaPLe	70.72	64.07	49.15	50.90	76.98
OrthSR	70.83	63.8	**49.3**	**51.37**	**77.4**

Table 3: Ablations of our proposed components. Results are averaged over 11 datasets. HM refers to harmonic mean.

Method	Base Acc.	Novel Acc.	HM
1: Final ***OrthSR***	84.16	76.55	80.02
2: ✓ Image Encoder	81.76	75.41	78.46
3: ✓ Text Encoder	80.70	76.19	78.38
4: - $\mathcal{L}_{\text{kl}}$	83.52	75.09	79.08
5: - cutout	81.75	76.55	79.06

4.2 Comparison with other methods

Base-to-base/base-to-new generalization. In this section, we compare the results of our approach over the ones that commonly use prompt learning or LoRA finetuning. As can be seen in Table 1, our approach obtains 84.16% , 76.55% and 80.02% Acc. for the averaged 11 datasets in terms of validation on base, new and HM. More importantly, our method surpasses the comparative $LoRA_{CLIP}$ with 2.74%, 6.15% and 4.95% of base, novel and HM evaluation, which further demonstrates the ***OrthSR*** is capable of not only efficiently adapting to task-specific task but also leading to generalizability preservation, thanks to the norm-preserving property of orthogonal finetuning. And these results further presents the prevalent $LoRA$ method potentially tends to prioritize task-specific knowledge and results in task overfitting issues while ours has no such issues, especially for the few-shot image recognition task. Meanwhile, our approach reports consistent superorities beyond the conventional prompt learning methods, VPT and IVLP, better illustrate the effectiveness of our approach. When compared with competing MaPLe [38] and PromptSRC [39] which utilize complex strategies to enhance prompt tuning, our method still behaves better generalizability, obtaining highest accuracy on evaluation with 76.55% for new classes and 80.02% for HM.

Cross-dataset transfer. For evaluating the cross-dataset tranfer, we train our approach on ImageNet [69] and then directly evaluate it on the other datasets without any domain-specific finetuning or adaptation. We compare cross-dataset performance with existing methods in Table 4. In comparison with CoOp [91] and CoCoOp [90], our proposed ***OrthSR*** presents better generalization performance in 9/10 and 5/10 datasets, respectively. Importantly, our approach exceeds $LoRA_{CLIP}$ in 9/10 datasets and shows obvious advantages among these dataset, which further demonstrates that our methods retains stronger zero-shot generalizability. Meanwhile, compared with the prompt tuning methods MaPLe [38] and PromptSRC [39], we obtain 7/10 and 6/10 better generalization performance while not introducing any tunable parameters after training (0 *v.s.* 3.55MB and 0 *v.s* 46KB, respectively) and no complicated training strategy tailored to struggle with the generalizability preservation.

Domain generalization. Table 2 reports the results of ***OrthSR*** and other methods on out-of-distribution datasets. Following the common methods, we train our model and directly evaluate on other datasets. We can observe that our method consistently surpasses $LoRA_{CLIP}$ on all datasets, while obtaining 3/4 superiority with CoOp and CoCoOp. Interestingly, prompt-based VPT illustrates inferior performance in 4/4 datasets to ours, while ours gains 2/4 better generlization evaluation beyond MaPLe [38]. This suggests that our orthogonal tuning with simple yet effective cross-regularization enables the finetuned model favor better generalization for datasets with domain shifts.

4.3 Ablations and analysis

Orthogonal tuning choice of encoder. In Table 3, we conduct experiments to to showcase which encoder, *i.e.,* image encoder or text encoder, should be introduced with the proposed orthogonal tuning. As can be observed that only utilizing single encoder of CLIP model presents lower performance on both base, novel and HM metrics while both encoders equipped with orthogonal finetuning obtain the best result, compared among row1/2/3.

Loss ablation. Compared among row 1/4/5 in Table 3, we found that removing logits distillation loss causes significant degradation on the *Novel/New* classes and HM metrics, which illustrates that there

Table 4: Performance comparison on the cross-dataset transfer setting.

	Source	Target									
	ImageNet	Caltech101	Oxford_Pets	StanfordCars	Flowers102	Food101	FGVCAircraft	SUN397	DTD	EuroSAT	UCF101
$LoRA_{CLIP}$	69.70	91.70	89.13	59.53	68.77	82.13	23.80	65.03	44.83	45.53	65.83
CoOp	**71.51**	93.70	89.14	64.51	68.71	85.30	18.47	64.15	41.92	46.39	66.55
CoCoOp	71.02	**94.43**	90.14	65.32	71.88	86.06	22.94	**67.36**	45.73	45.37	68.21
MaPLe	70.72	93.53	**90.49**	65.57	**72.23**	86.20	**24.74**	67.01	46.49	**48.06**	68.69
PromptSRC	71.27	93.60	90.25	65.70	70.25	86.15	23.90	67.10	**46.87**	45.50	68.75
OrthSR	70.83	94.07	89.63	65.63	71.40	**86.53**	24.13	67.23	46.73	42.33	**69.17**

Table 5: Complexity analysis over various methods. We report the number of trainable parameters (#Params) and frames per second (#fps).

Methods	CoOp	CoCoOp	VPT	PLOT	MAPLE	***OrthSR***
#Params	2,048	35,360	13,824	8,192	3,555,072	43450368
#fps	**645**	37	152	583	282	**645**

are some kind of deviation away from the pretrained model, proving that necessitates regularization to guide the finetuning. After using logits distillation, $\mathcal{L}_{kl}$, we get improved on both the Base and Novel classes, by 0.64% and 1.46%, respecitvely. Note that we derive such distillation guidance from the pretrained model only in a bypass manner, instead of seeking for extra data synthesis or heavy large-language model prior knowledge auxiliary.

Complexity analysis. Since our proposed orthogonal tuning method shares similar idea with $LoRA$ adapting VLMs into downstream scenarios via pretrained weights finetuning, it is necessary to demonstrate the computation cost during the training and inference phases. We therefore test and summarize the number of trainable parameters (#Params) and inference latency (#fps) in Table 5. We can see that though our approach needs the most number of trainable parameters since we leverage both two encoders to be injected with orthogonal tuning matrices for each fully-connected layer within Feed-Forward-Network, our approach needs the same inference latency with the baseline, CoOp, achieving the fastest 645 fps while having significantly better few-shot recognition and generalization performance. More ablative studies please refer to our Appendix A.

5 Conclusions

This paper proposes a novel and efficient method for adapting pretrained VLM weights, ***OrthSR***, for specific downstream tasks (*e.g.,* few-shot image recognition). To explore an effective fine-tuning approach not suffering from task overfitting issues under a data-efficient setting, we propose an orthogonal fine-tuning method for efficiently updating pretrained weights. Optimized by the constraint with Cayley parameterization during training, the fine-tuned CLIP model is capable of maintaining minimal and same-level of hyperspherical energy as the pretrained model owing to norm-preserving property, leading to better robustness and generalizability for task-specific scenarios. Meanwhile, a self-regularization strategy is designed to enforce the model not to deviate far away from the pretrained one within a bypass manner. Additionally, we first explore attentive CutOut data augmentation to enable the fine-tuned model to learn better task-specific knowledge on a small data set. Finally, extensive experiments demonstrate the training efficiency and generalizability preservation of our approach and showcase competitive performance on three generalization evaluations, shedding new light on the future works for this few-shot tuning task.

Limitations and future improvements. Despite the competitive generalization performance our approach obtains, there are still several limitations to be further delved into exploration. First, our method presents marginal advantages on *cross-dataset transfer* or *domain generalization* evaluations, although we exhibit competitive performance under *base-to-base/base-to-new* setting. Moreover, there are still future improvements on how to efficiently lower the tunable parameters during the training phase, and remaining an interesting direction on how to leverage theoretical analysis to decompose or disentangle the VLMs to seek out the potential manifold space that allows us to inject task-specific knowledge without sacrificing zero-shot generalizability.

References

[1] Martin Arjovsky, Amar Shah, and Yoshua Bengio. Unitary evolution recurrent neural networks. In *ICML*, pp. 1120–1128. PMLR, 2016.

[2] Hyojin Bahng, Ali Jahanian, Swami Sankaranarayanan, and Phillip Isola. Exploring visual prompts for adapting large-scale models. *arXiv preprint arXiv:2203.17274*, 2022.

[3] H. Bangalath, M. Maaz, M. Khattak, S. Khan, and F. Shahbaz Khan. Bridging the gap between object and image-level representations for open-vocabulary detection. *NeurIPS*, 2022.

[4] Yoshua Bengio, Patrice Simard, and Paolo Frasconi. Learning long-term dependencies with gradient descent is difficult. *IEEE transactions on neural networks*, 5(2):157–166, 1994.

[5] Lukas Bossard, Matthieu Guillaumin, and Luc Van Gool. Food-101–mining discriminative components with random forests. In *ECCV*, pp. 446–461. Springer, 2014.

[6] L. Boyi, W. Kilian, B. Serge, K. Vladlen, and R. Rene. Language-driven semantic segmentation. In *ICLR*, 2022.

[7] Andrew Brock, Theodore Lim, James M Ritchie, and Nick Weston. Neural photo editing with introspective adversarial networks. In *ICLR*, 2017.

[8] Tom Brown, Benjamin Mann, Nick Ryder, Melanie Subbiah, Jared D Kaplan, Prafulla Dhariwal, Arvind Neelakantan, Pranav Shyam, Girish Sastry, Amanda Askell, et al. Language models are few-shot learners. In *NeurIPS*, volume 33, pp. 1877–1901, 2020.

[9] Beidi Chen, Weiyang Liu, Zhiding Yu, Jan Kautz, Anshumali Shrivastava, Animesh Garg, and Animashree Anandkumar. Angular visual hardness. In *ICML*, pp. 1637–1648. PMLR, 2020.

[10] Guangyi Chen, Weiran Yao, Xiangchen Song, Xinyue Li, Yongming Rao, and Kun Zhang. Plot: Prompt learning with optimal transport for vision-language models. In *ICLR*, 2023.

[11] Zhenyuan Chen, Lingfeng Yang, Shuo Chen, Zhaowei Chen, Jiajun Liang, and Xiang Li. Revisiting prompt pretraining of vision-language models. *arXiv preprint arXiv:2409.06166*, 2024.

[12] Cheng Cheng, Lin Song, Ruoyi Xue, Hang Wang, Hongbin Sun, Yixiao Ge, and Ying Shan. Meta-adapter: An online few-shot learner for vision-language model. In *NeurIPS*, 2023.

[13] M. Cherti, R. Beaumont, R. Wightman, M. Wortsman, G. Ilharco, C. Gordon, C. Schuhmann, L. Schmidt, and J. Jitsev. Reproducible scaling laws for contrastive language-image learning. In *CVPR*, 2023.

[14] Eulrang Cho, Jooyeon Kim, and Hyunwoo J Kim. Distribution-aware prompt tuning for vision-language models. In *ICCV*, pp. 22004–22013, 2023.

[15] Mircea Cimpoi, Subhransu Maji, Iasonas Kokkinos, Sammy Mohamed, and Andrea Vedaldi. Describing textures in the wild. In *CVPR*, pp. 3606–3613, 2014.

[16] Tim Dettmers, Artidoro Pagnoni, Ari Holtzman, and Luke Zettlemoyer. Qlora: Efficient finetuning of quantized llms. In *NeurIPS*, volume 36, 2024.

[17] Jacob Devlin, Ming-Wei Chang, Kenton Lee, and Kristina Toutanova. Bert: Pre-training of deep bidirectional transformers for language understanding. In *ACL*, 2019.

[18] Jian Ding, Nan Xue, Gui-Song Xia, and Dengxin Dai. Decoupling zero-shot semantic segmentation. In *CVPR*, pp. 11583–11592, 2022.

[19] Alexey Dosovitskiy, Lucas Beyer, Alexander Kolesnikov, Dirk Weissenborn, Xiaohua Zhai, Thomas Unterthiner, Mostafa Dehghani, Matthias Minderer, Georg Heigold, Sylvain Gelly, et al. An image is worth 16x16 words: Transformers for image recognition at scale. In *ICLR*, 2020.

[20] Li Fei-Fei. Learning generative visual models from few training examples. In *CVPR-W*, 2004.

[21] Chengjian Feng, Yujie Zhong, Zequn Jie, Xiangxiang Chu, Haibing Ren, Xiaolin Wei, Weidi Xie, and Lin Ma. Promptdet: Towards open-vocabulary detection using uncurated images. In *ECCV*, pp. 701–717. Springer, 2022.

[22] Peng Gao, Shijie Geng, Renrui Zhang, Teli Ma, Rongyao Fang, Yongfeng Zhang, Hongsheng Li, and Yu Qiao. Clip-adapter: Better vision-language models with feature adapters. *IJCV*, 132 (2):581–595, 2024.

[23] Tianyu Gao, Adam Fisch, and Danqi Chen. Making pre-trained language models better few-shot learners. In *ACL*, 2021.

[24] Xavier Glorot and Yoshua Bengio. Understanding the difficulty of training deep feedforward neural networks. In *AISTATS*, pp. 249–256. JMLR Workshop and Conference Proceedings, 2010.

[25] Xiuye Gu, Tsung-Yi Lin, Weicheng Kuo, and Yin Cui. Open-vocabulary detection via vision and language knowledge distillation. *arXiv preprint arXiv:2104.13921*, 2021.

[26] Kaiming He, Xiangyu Zhang, Shaoqing Ren, and Jian Sun. Deep residual learning for image recognition. In *CVPR*, pp. 770–778, 2016.

[27] Kaiming He, Xinlei Chen, Saining Xie, Yanghao Li, Piotr Dollár, and Ross Girshick. Masked autoencoders are scalable vision learners. In *CVPR*, pp. 16000–16009, 2022.

[28] Patrick Helber, Benjamin Bischke, Andreas Dengel, and Damian Borth. Eurosat: A novel dataset and deep learning benchmark for land use and land cover classification. *IEEE J-STARS*, 12(7):2217–2226, 2019.

[29] Kyle Helfrich, Devin Willmott, and Qiang Ye. Orthogonal recurrent neural networks with scaled cayley transform. In *ICML*, pp. 1969–1978. PMLR, 2018.

[30] Dan Hendrycks, Steven Basart, Norman Mu, Saurav Kadavath, Frank Wang, Evan Dorundo, Rahul Desai, Tyler Zhu, Samyak Parajuli, Mike Guo, et al. The many faces of robustness: A critical analysis of out-of-distribution generalization. In *ICCV*, pp. 8340–8349, 2021.

[31] Dan Hendrycks, Kevin Zhao, Steven Basart, Jacob Steinhardt, and Dawn Song. Natural adversarial examples. In *CVPR*, pp. 15262–15271, 2021.

[32] Neil Houlsby, Andrei Giurgiu, Stanislaw Jastrzebski, Bruna Morrone, Quentin De Laroussilhe, Andrea Gesmundo, Mona Attariyan, and Sylvain Gelly. Parameter-efficient transfer learning for nlp. In *ICML*, pp. 2790–2799. PMLR, 2019.

[33] Edward J Hu, Yelong Shen, Phillip Wallis, Zeyuan Allen-Zhu, Yuanzhi Li, Shean Wang, Lu Wang, and Weizhu Chen. LoRA: Low-rank adaptation of large language models. In *ICLR*, 2022. URL `https://openreview.net/forum?id=nZeVKeeFYf9`.

[34] Lei Huang, Xianglong Liu, Bo Lang, Adams Yu, Yongliang Wang, and Bo Li. Orthogonal weight normalization: Solution to optimization over multiple dependent stiefel manifolds in deep neural networks. In *AAAI*, volume 32, 2018.

[35] Lei Huang, Li Liu, Fan Zhu, Diwen Wan, Zehuan Yuan, Bo Li, and Ling Shao. Controllable orthogonalization in training dnns. In *CVPR*, pp. 6429–6438, 2020.

[36] C. Jia, Y. Yang, Y. Xia, Y.-T. Chen, Z. Parekh, H. Pham, Q. Le, Y.-H. Sung, Z. Li, and T. Duerig. Scaling up visual and vision-language representation learning with noisy text supervision. In *ICML*, 2021.

[37] Menglin Jia, Luming Tang, Bor-Chun Chen, Claire Cardie, Serge Belongie, Bharath Hariharan, and Ser-Nam Lim. Visual prompt tuning. In *ECCV*, pp. 709–727. Springer, 2022.

[38] Muhammad Uzair Khattak, Hanoona Rasheed, Muhammad Maaz, Salman Khan, and Fahad Shahbaz Khan. Maple: Multi-modal prompt learning. In *CVPR*, pp. 19113–19122, 2023.

[39] Muhammad Uzair Khattak, Syed Talal Wasim, Muzammal Naseer, Salman Khan, Ming-Hsuan Yang, and Fahad Shahbaz Khan. Self-regulating prompts: Foundational model adaptation without forgetting. In *CVPR*, pp. 15190–15200, 2023.

[40] Jonathan Krause, Michael Stark, Jia Deng, and Li Fei-Fei. 3d object representations for fine-grained categorization. In *ICCV-W*, pp. 554–561, 2013.

[41] Dongjun Lee, Seokwon Song, Jihee Suh, Joonmyeong Choi, Sanghyeok Lee, and Hyunwoo J Kim. Read-only prompt optimization for vision-language few-shot learning. In *ICCV*, pp. 1401–1411, 2023.

[42] Brian Lester, Rami Al-Rfou, and Noah Constant. The power of scale for parameter-efficient prompt tuning. *arXiv preprint arXiv:2104.08691*, 2021.

[43] Mario Lezcano-Casado and David Martınez-Rubio. Cheap orthogonal constraints in neural networks: A simple parametrization of the orthogonal and unitary group. In *ICML*, pp. 3794–3803. PMLR, 2019.

[44] Juncheng Li, Minghe Gao, Longhui Wei, Siliang Tang, Wenqiao Zhang, Mengze Li, Wei Ji, Qi Tian, Tat-Seng Chua, and Yueting Zhuang. Gradient-regulated meta-prompt learning for generalizable vision-language models. In *ICCV*, pp. 2551–2562, 2023.

[45] Shuai Li, Kui Jia, Yuxin Wen, Tongliang Liu, and Dacheng Tao. Orthogonal deep neural networks. *T-PAMI*, 43(4):1352–1368, 2019.

[46] Xiang Lisa Li and Percy Liang. Prefix-tuning: Optimizing continuous prompts for generation. *arXiv preprint arXiv:2101.00190*, 2021.

[47] Yanghao Li, Haoqi Fan, Ronghang Hu, Christoph Feichtenhofer, and Kaiming He. Scaling language-image pre-training via masking. In *CVPR*, pp. 23390–23400, 2023.

[48] Rongmei Lin, Weiyang Liu, Zhen Liu, Chen Feng, Zhiding Yu, James M Rehg, Li Xiong, and Le Song. Regularizing neural networks via minimizing hyperspherical energy. In *CVPR*, pp. 6917–6927, 2020.

[49] Pengfei Liu, Weizhe Yuan, Jinlan Fu, Zhengbao Jiang, Hiroaki Hayashi, and Graham Neubig. Pre-train, prompt, and predict: A systematic survey of prompting methods in natural language processing. *ACM Computing Surveys*, 55(9):1–35, 2023.

[50] Shih-Yang Liu, Chien-Yi Wang, Hongxu Yin, Pavlo Molchanov, Yu-Chiang Frank Wang, Kwang-Ting Cheng, and Min-Hung Chen. Dora: Weight-decomposed low-rank adaptation. In *ICML*, 2024.

[51] Weiyang Liu, Yan-Ming Zhang, Xingguo Li, Zhiding Yu, Bo Dai, Tuo Zhao, and Le Song. Deep hyperspherical learning. In *NeurIPS*, volume 30, 2017.

[52] Weiyang Liu, Rongmei Lin, Zhen Liu, Lixin Liu, Zhiding Yu, Bo Dai, and Le Song. Learning towards minimum hyperspherical energy. In *NeurIPS*, volume 31, 2018.

[53] Weiyang Liu, Zhen Liu, Zhiding Yu, Bo Dai, Rongmei Lin, Yisen Wang, James M Rehg, and Le Song. Decoupled networks. In *CVPR*, pp. 2771–2779, 2018.

[54] Weiyang Liu, Rongmei Lin, Zhen Liu, James M Rehg, Liam Paull, Li Xiong, Le Song, and Adrian Weller. Orthogonal over-parameterized training. In *CVPR*, pp. 7251–7260, 2021.

[55] Yuning Lu, Jianzhuang Liu, Yonggang Zhang, Yajing Liu, and Xinmei Tian. Prompt distribution learning. In *CVPR*, pp. 5206–5215, 2022.

[56] Subhransu Maji, Esa Rahtu, Juho Kannala, Matthew Blaschko, and Andrea Vedaldi. Fine-grained visual classification of aircraft. *arXiv preprint arXiv:1306.5151*, 2013.

[57] Shu Manli, Nie Weili, Huang De-An, Yu Zhiding, Goldstein Tom, Anandkumar Anima, and Xiao Chaowei. Test-time prompt tuning for zero-shot generalization in vision-language models. In *NeurIPS*, 2022.

[58] Tsendsuren Munkhdalai and Hong Yu. Meta networks. In *ICML*, pp. 2554–2563. PMLR, 2017.

[59] Yao Ni, Shan Zhang, and Piotr Koniusz. Pace: marrying generalization in parameter-efficient fine-tuning with consistency regularization. *arXiv preprint arXiv:2409.17137*, 2024.

[60] Maria-Elena Nilsback and Andrew Zisserman. Automated flower classification over a large number of classes. In *ICVGIP*, pp. 722–729. IEEE, 2008.

[61] Jinyoung Park, Juyeon Ko, and Hyunwoo J Kim. Prompt learning via meta-regularization. In *CVPR*, 2024.

[62] Omkar M Parkhi, Andrea Vedaldi, Andrew Zisserman, and CV Jawahar. Cats and dogs. In *CVPR*, pp. 3498–3505. IEEE, 2012.

[63] Clifton Poth, Hannah Sterz, Indraneil Paul, Sukannya Purkayastha, Leon Engländer, Timo Imhof, Ivan Vulić, Sebastian Ruder, Iryna Gurevych, and Jonas Pfeiffer. Adapters: A unified library for parameter-efficient and modular transfer learning. In *EMNLP*, pp. 149–160, Singapore, December 2023. Association for Computational Linguistics. URL `https://aclanthology.org/2023.emnlp-demo.13`.

[64] Haozhi Qi, Chong You, Xiaolong Wang, Yi Ma, and Jitendra Malik. Deep isometric learning for visual recognition. In *ICML*, pp. 7824–7835. PMLR, 2020.

[65] Zeju Qiu, Weiyang Liu, Haiwen Feng, Yuxuan Xue, Yao Feng, Zhen Liu, Dan Zhang, Adrian Weller, and Bernhard Schölkopf. Controlling text-to-image diffusion by orthogonal finetuning. In *NeurIPS*, volume 36, pp. 79320–79362, 2023.

[66] A. Radford, J. Kim, C. Hallacy, et al. Learning transferable visual models from natural language supervision. In *ICML*, 2021.

[67] Yongming Rao, Wenliang Zhao, Guangyi Chen, Yansong Tang, Zheng Zhu, Guan Huang, Jie Zhou, and Jiwen Lu. Denseclip: Language-guided dense prediction with context-aware prompting. In *CVPR*, pp. 18082–18091, 2022.

[68] Benjamin Recht, Rebecca Roelofs, Ludwig Schmidt, and Vaishaal Shankar. Do imagenet classifiers generalize to imagenet? In *ICML*, pp. 5389–5400. PMLR, 2019.

[69] O. Russakovsky, J. Deng, H. Su, J. Krause, S. Satheesh, S. Ma, Z. Huang, A. Karpathy, A. Khosla, M. Bernstein, et al. Imagenet large scale visual recognition challenge. *IJCV*, 2015.

[70] Jameel Hassan Abdul Samadh, Hanan Gani, Noor Hazim Hussein, Muhammad Uzair Khattak, Muzammal Naseer, Fahad Khan, and Salman Khan. Align your prompts: Test-time prompting with distribution alignment for zero-shot generalization. In *NeurIPS*, 2023.

[71] Manli Shu, Weili Nie, De-An Huang, Zhiding Yu, Tom Goldstein, Anima Anandkumar, and Chaowei Xiao. Test-time prompt tuning for zero-shot generalization in vision-language models. In *NeurIPS*, volume 35, pp. 14274–14289, 2022.

[72] Sahil Singla and Soheil Feizi. Skew orthogonal convolutions. In *ICML*, pp. 9756–9766. PMLR, 2021.

[73] Khurram Soomro, Amir Roshan Zamir, and Mubarak Shah. Ucf101: A dataset of 101 human actions classes from videos in the wild. *arXiv preprint arXiv:1212.0402*, 2012.

[74] Hugo Touvron, Thibaut Lavril, Gautier Izacard, Xavier Martinet, Marie-Anne Lachaux, Timothée Lacroix, Baptiste Rozière, Naman Goyal, Eric Hambro, Faisal Azhar, et al. Llama: Open and efficient foundation language models (2023). *arXiv preprint arXiv:2302.13971*, 2023.

[75] Ashish Vaswani, Noam Shazeer, Niki Parmar, Jakob Uszkoreit, Llion Jones, Aidan N Gomez, Łukasz Kaiser, and Illia Polosukhin. Attention is all you need. In *NeurIPS*, volume 30, 2017.

[76] Roman Vershynin. *High-dimensional probability: An introduction with applications in data science*, volume 47. Cambridge university press, 2018.

[77] Dongsheng Wang, Miaoge Li, Xinyang Liu, MingSheng Xu, Bo Chen, and Hanwang Zhang. Tuning multi-mode token-level prompt alignment across modalities. In *NeurIPS*, volume 36, 2023.

[78] Haohan Wang, Songwei Ge, Zachary Lipton, and Eric P Xing. Learning robust global representations by penalizing local predictive power. In *NeurIPS*, volume 32, 2019.

[79] Xudong Wang, Shufan Li, Konstantinos Kallidromitis, Yusuke Kato, Kazuki Kozuka, and Trevor Darrell. Hierarchical open-vocabulary universal image segmentation. In *NeurIPS*, volume 36, 2024.

[80] Scott Wisdom, Thomas Powers, John Hershey, Jonathan Le Roux, and Les Atlas. Full-capacity unitary recurrent neural networks. In *NeurIPS*, volume 29, 2016.

[81] Yongqin Xian, Bernt Schiele, and Zeynep Akata. Zero-shot learning-the good, the bad and the ugly. In *CVPR*, pp. 4582–4591, 2017.

[82] Jianxiong Xiao, James Hays, Krista A Ehinger, Aude Oliva, and Antonio Torralba. Sun database: Large-scale scene recognition from abbey to zoo. In *CVPR*, pp. 3485–3492. IEEE, 2010.

[83] Di Xie, Jiang Xiong, and Shiliang Pu. All you need is beyond a good init: Exploring better solution for training extremely deep convolutional neural networks with orthonormality and modulation. In *CVPR*, pp. 6176–6185, 2017.

[84] Lu Yuan, Dongdong Chen, Yi-Ling Chen, Noel Codella, Xiyang Dai, Jianfeng Gao, Houdong Hu, Xuedong Huang, Boxin Li, Chunyuan Li, et al. Florence: A new foundation model for computer vision. *arXiv preprint arXiv:2111.11432*, 2021.

[85] Yuhang Zang, Wei Li, Kaiyang Zhou, Chen Huang, and Chen Change Loy. Open-vocabulary detr with conditional matching. In *ECCV*, pp. 106–122. Springer, 2022.

[86] Yuhang Zang, Wei Li, Kaiyang Zhou, Chen Huang, and Chen Change Loy. Unified vision and language prompt learning. *arXiv preprint arXiv:2210.07225*, 2022.

[87] Xiaohua Zhai, Xiao Wang, Basil Mustafa, Andreas Steiner, Daniel Keysers, Alexander Kolesnikov, and Lucas Beyer. Lit: Zero-shot transfer with locked-image text tuning. In *CVPR*, pp. 18123–18133, 2022.

[88] Renrui Zhang, Rongyao Fang, Wei Zhang, Peng Gao, Kunchang Li, Jifeng Dai, Yu Qiao, and Hongsheng Li. Tip-adapter: Training-free clip-adapter for better vision-language modeling. In *ECCV*, 2022.

[89] Yuhao Zhang, Hang Jiang, Yasuhide Miura, Christopher D Manning, and Curtis P Langlotz. Contrastive learning of medical visual representations from paired images and text. In *MLHC*, pp. 2–25. PMLR, 2022.

[90] Kaiyang Zhou, Jingkang Yang, Chen Change Loy, and Ziwei Liu. Conditional prompt learning for vision-language models. In *CVPR*, 2022.

[91] Kaiyang Zhou, Jingkang Yang, Chen Change Loy, and Ziwei Liu. Learning to prompt for vision-language models. *IJCV*, 2022.

[92] Beier Zhu, Yulei Niu, Yucheng Han, Yue Wu, and Hanwang Zhang. Prompt-aligned gradient for prompt tuning. In *ICCV*, pp. 15659–15669, 2023.

A Appendix / supplemental material

A.1 More implementation details

Besides the implementation details in our main paper, we provide more details in Table 6.

Table 6: Hyperparameter setting used in our experiments.

Hyperparameters	Values
Batch Size	4
Input Size	224×224
Input Interpolation	"Bicubic"
Input Pixel Mean	$[0.48145466, 0.4578275, 0.40821073]$
Input Pixel STD	$[0.26862954, 0.26130258, 0.27577711]$
Transforms	["random resized crop", "random filp", "normalize"]
Optimizer	SGD
Learning Rate	0.00001
LR Scheduler	"cosine"
Warmup Epoch	1
Warmup Type	"constant"
Warmup LR	$1e$-6
Backbone	ViT-B/16
Number of Textual Prompts	4
Number of Visual Prompts	4
Learnable Prompt Length	2
Fixed Prompt Length	2
weight of cross-entropy loss λ_1	1.5
weight of *Kullback-Leibler* loss λ_2	1.2
patch number for Cutout inference (ViT-B/16)	randomly sample one from $[5, 6, 7, 8, 9]$
Prompt Initialization	"a photo of a"
Precision	"fp16"

A.2 Evaluation metrics

Among all our experiments, we report top_1 accuracy for each dataset. In *base-to-base/base-to-new* generalization, the top_1 accuracy is measured on base classes and new classes, respectively. We then calculate the harmonic mean (HM) between the base and new class accuracy to show the generalization trade-off [81], using $HM = \frac{2 \times base \times new}{base + new}$. In *domain generalization*, and *cross-dataset transfer* settings, we measure $top-1$ accuracy on the test set of each dataset with the same split provided by CoOp [91] following other related works.

A.3 More dataset descriptions

We throughly conduct our method on publicly available 15 image recognition datasets across 4 common generalizability evaluation settings: ImageNet [69] and Caltech101 [20] for generic objects classification, Oxford_Pets [62], StanfordCars [40], Flowers102 [60], Food101 [5] and FGVCAircraft [56] for fine-grained classification, SUN397 [82] for scene recognition, DTD [15] for texture classification, EuroSAT [28] for satellite imagery recognition and UCF101 [73] for action recognition; datasets with apparent domain shifts ImageNetV2 [68], ImageNet-Sketch [78], ImageNet-A [31] and ImageNet-R [30]. We make a summary in terms of data statistics in Table 7.

A.4 Loss balancing hyper-parameters sensitivity ablations

In our main paper, the overall training loss $\mathcal{L}_{final}$ is:

$$\mathcal{L}_{\text{final}} = \lambda_1(\mathcal{L}_{ce} + \mathcal{L}_{cutout\_ce}) + \lambda_2(\mathcal{L}_{kl} + \mathcal{L}_{cutout\_kl}) \tag{12}$$

Table 7: Summary of all 15 datasets. N/A denotes that we do not use the corresponding training or validation sets, which will be used to conduct generalizability evaluation only.

Dataset	Domains	**#Classes**	**#Train**	**#Val**	**#Test**
ImageNet	generic classification	1000	1.28M	N/A	50,000
Caltech101	generic classification	100	4,128	1,649	2,465
OxfordPets	fine-grained classification	37	2,944	736	3,669
StanfordCars	fine-grained classification	196	6,509	1,635	8,041
Flowers102	fine-grained classification	102	4,093	1,633	2,463
Food101	fine-grained classification	101	50,500	20,200	30,300
FDVCAircraft	fine-grained classification	100	3,334	3,333	3,333
SUN397	scene recognition	397	15,880	3,970	19,850
UCF101	action recognition	101	7,639	1,808	3,783
DTD	texture recognition	47	2,820	1,128	1,692
EuroSAT	satellite recognition	10	13,500	5,400	8,100
ImageNetV2	generic classification	1000	N/A	N/A	10,000
ImageNet-Sketch	sketch classification	1000	N/A	N/A	50,889
ImageNet-A	generic classification	200	N/A	N/A	7,500
ImageNet-R	generic classification	200	N/A	N/A	30,000

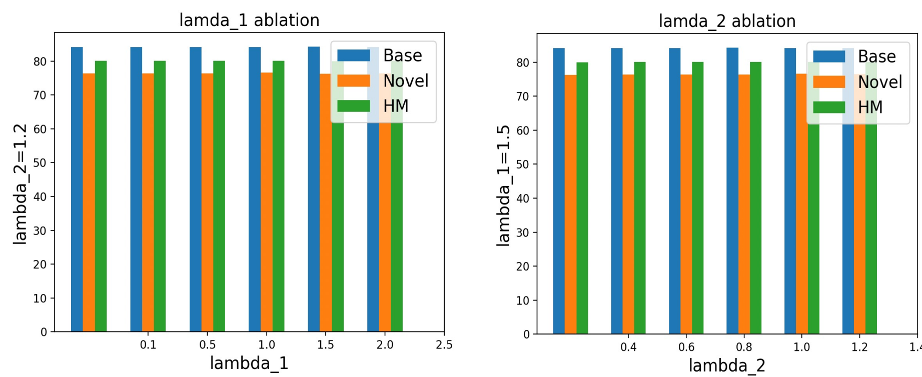

(a) fix λ_2 = 1.2 (b) fix λ_1 = 1.5

Figure 3: Ablations in terms of λ_1 and λ_2.

In this section, we conduct ablative studies on hyper-parameters, λ_1 and λ_2 in Fig 3. The figure shows that the overall training is robust to both the hyper-parameters, λ_1 and λ_2.

B Theoretical Proof

Following previous works [11; 59], this section provides detailed proofs for the Theorem in Sec. 3.6. Notably, we propose to utilize attentive CutOut data augmentation to implicitly increase the sample number and make use of pre-trained model as generalization *anchor* to maintain the generalization error bound, which is different from [11]. We introduce the following lemmas for proving our Theorem.

Lemma 1(McDiarmid's Inequality [76]). *Consider independent random variables* $v_1, v_2, \cdots, v_n \in \mathcal{V}$ *and a function* $\phi : \mathcal{V}^n \to \mathbb{R}$*. Suppose that for all* $v_1, v_2, \cdots, v_n$ *and* $v_i{}' \in \mathcal{V}\,(i = 1, 2, \cdots, n)$*, the function satisfies*

$$\left|\phi\left(v_1, \cdots, V_{i-1}, V_i, V_{i+1}, \cdots, V_n\right) - \phi\left(v_1, \cdots, V_{i-1}, v_i{}', V_{i+1}, \cdots, V_n\right)\right| \le c_i, \tag{13}$$

and then it holds that

$$\mathcal{P}\left\{\phi\left(v_1, v_2, \cdots, v_n\right) - \mathbb{E}_{v_1, v_2, \cdots, v_n}\left(\phi\left(v_1, v_2, \cdots, v_n\right)\right) > \mu\right\} \le e^{-\frac{2\mu^2}{\sum_{i=1}^{n} c_i^2}}. \tag{14}$$

The proof of Theorem 1. is given as follows.

Theorem 1. *Assume that Θ^* is the solution to OrthSR. Then we have that for any $0 < \varepsilon < 1$ with probability $1 - \varepsilon$,*

$$\epsilon(\Theta^*) - \bar{\epsilon}_\chi(\Theta^*) \leq X^* \sqrt{\frac{2\ln(1/\delta)}{N}} + \frac{C''}{\lambda^{2\alpha}\sqrt{N}}.$$

where $\epsilon(\Theta^*)$ is the true error. $\bar{\epsilon}_\chi(\Theta^*)$ is the empirical error. X^* is the upper bound of the loss function L. N is the number of training samples. λ is our introduced regularization parameter. $\alpha > 0$. δ is a probability parameter. C'' encompasses constants from the Rademacher complexity bound.

Proof. The generalization error is defined as:

$$\epsilon(\Theta) = \mathbb{E}_{(x,y)\sim D}\left[L(s_\Theta(x), y)\right]$$

where Θ represents the model parameters, $L(s_\Theta(x), y)$ is the loss function, and D is the true data distribution.

The empirical error is:

$$\bar{\epsilon}_\chi(\Theta) = \frac{1}{N}\sum_{i=1}^{N} L(s_\Theta(x_i), y_i)$$

where $\chi = \{(x_i, y_i)\}_{i=1}^N$ is the training set, and N is the sample size.

We use McDiarmid's inequality to control the deviation between empirical error and true error. The inequality states:

$$P\left(f(X_1, \ldots, X_n) - \mathbb{E}[f(X_1, \ldots, X_n)] > t\right) \leq \exp\left(-\frac{2t^2}{\sum_{i=1}^n c_i^2}\right)$$

where $X_1, X_2, \ldots, X_n$ are independent random variables, and $f(X_1, \ldots, X_n)$ is a function of these variables. When one sample in the training set changes, the maximum change in the empirical error is:

$$\Delta = \bar{\epsilon}_\chi(\Theta) - \bar{\epsilon}_{\chi'}(\Theta)$$

The change in empirical error is bounded by $\frac{c}{N}$, where c is the upper bound on the difference in the loss function:

$$|L(s_\Theta(x), y) - L(s_\Theta(x'), y')| \leq c$$

Applying McDiarmid's inequality with the bound $\frac{c}{N}$, we obtain the following bound:

$$P\left(\epsilon(\Theta) - \bar{\epsilon}_\chi(\Theta) > t\right) \leq \exp\left(-\frac{2Nt^2}{c^2}\right)$$

We introduce the Rademacher complexity $R_N(L)$, which measures the complexity of the model:

$$R_N(L) = \mathbb{E}_{\sigma,\chi}\left[\sup_{\Theta\in\mathcal{H}} \frac{1}{N}\sum_{i=1}^{N} \sigma_i L(s_\Theta(x_i), y_i)\right]$$

The generalization error bound becomes:

$$\epsilon(\Theta) \leq \bar{\epsilon}_\chi(\Theta) + 2R_N(L) + X^*\sqrt{\frac{2\ln(1/\delta)}{N}}$$

where: $\bar{\epsilon}_\chi(\Theta)$ is the empirical error. $2R_N(L)$ is the Rademacher complexity term. $X^*\sqrt{\frac{2\ln(1/\delta)}{N}}$ is the variance term that decreases as the sample size N increases. To further reduce the generalization error, we introduce the regularization term L_{KD} (Knowledge Distillation Loss) in Eq. 10, which limits the complexity of the model. The objective function of our OrthSR is:

$$\min_{\Theta} \left(L_{CE} + \lambda L_{KD} \right)$$

where L_{CE} is the cross-entropy loss for measuring the fit of the model. L_{KD} is the knowledge distillation loss, reducing the difference between student and teacher models. λ controls the trade-off between the two losses. To understand why the Rademacher complexity $R_N(L)$ is reduced under the regularization term, we analyze how regularization influences the hypothesis space $\mathcal{H}$ and, consequently, the complexity of the loss function class.

The Rademacher complexity $R_N(L)$ measures the richness of the loss class $\mathcal{L} = \{L(s_\Theta(x), y) : \Theta \in \mathcal{H}\}$ by evaluating how well it can fit random noise. It is defined as:

$$R_N(L) = \mathbb{E}_{\sigma, \chi} \left[\sup_{\Theta \in \mathcal{H}} \frac{1}{N} \sum_{i=1}^{N} \sigma_i L(s_\Theta(x_i), y_i) \right],$$

where σ_i are independent Rademacher variables taking values ± 1 with equal probability.

Regularization introduces a penalty term λL_{KD} in the objective function:

$$\min_{\Theta} \left(L_{CE} + \lambda L_{KD} \right).$$

This penalty discourages complex models by imposing a cost on large parameter values or deviations from the teacher model in knowledge distillation. As a result, the effective hypothesis space $\mathcal{H}_\lambda$ becomes smaller or more restricted because models with high complexity are penalized.

Mathematically, stronger regularization (larger λ) enforces tighter constraints on Θ, effectively reducing the norm or other measures of complexity of the model parameters. We assume that through regularization, the model parameters satisfy the following constraint:

$$\|\Theta\| \leq \frac{C}{\lambda^\beta},$$

where C and $\beta > 0$ are constants.

Under this constraint, and assuming that the loss function L is Lipschitz continuous with Lipschitz constant L_0, the Rademacher complexity can be bounded as:

$$R_N(L) \leq \frac{L_0 C'}{\lambda^\beta \sqrt{N}},$$

where C' is another constant.

Substituting this bound into the generalization error bound, we have:

$$\epsilon(\Theta^*) - \bar{\epsilon}_\chi(\Theta^*) \leq X^* \sqrt{\frac{2\ln(1/\delta)}{N}} + \frac{1}{\lambda^\alpha} \cdot R_N(L) \leq X^* \sqrt{\frac{2\ln(1/\delta)}{N}} + \frac{L_0 C'}{\lambda^{\alpha+\beta}\sqrt{N}}.$$

To ensure consistency in the exponents of λ, we set:

$$\alpha = \beta > 0.$$

Therefore, the generalization error bound becomes:

$$\epsilon(\Theta^*) - \bar{\epsilon}_\chi(\Theta^*) \leq X^* \sqrt{\frac{2\ln(1/\delta)}{N}} + \frac{C''}{\lambda^{2\alpha}\sqrt{N}},$$

where $C'' = L_0 C'$ is a constant.

This inequality shows that $R_N(L)$ decreases as λ increases, since $\alpha > 0$. By reducing $R_N(L)$ through regularization, we tighten the generalization error bound:

$$\epsilon(\Theta^*) - \bar{\epsilon}_{\chi}(\Theta^*) \leq X^* \sqrt{\frac{2\ln(1/\delta)}{N}} + \frac{C''}{\lambda^{2\alpha}\sqrt{N}}.$$

In summary, the regularization term reduces the Rademacher complexity $R_N(L)$ by limiting the capacity of the hypothesis space $\mathcal{H}$. This reduction leads to better generalization performance by preventing overfitting and tightening the generalization error bound.

$\square$